Toxicological Sciences
ToxSci Advance Access published January 12, 2011

Selective phthalate activation of naturally occurring human constitutive androstane receptor splice variants and the pregnane X receptor

Joshua G. DeKeyser*‡, Elizabeth M. Laurenzana*§, Eric C. Peterson†, Tao Chen* and Curtis J. Omiecinski*

*Center for Molecular Toxicology and Carcinogenesis, Department of Veterinary and Biomedical Sciences, 101 Life Sciences Building, Pennsylvania State University, University Park, PA 16802

†Department of Pharmacology and Toxicology, University of Arkansas for Medical Sciences, 4301 W. Markham St, Little Rock, AR 72205

Running head: Phthalate interaction with CAR and PXR

‡Current address: Amgen Pharmacokinetics and Drug Metabolism, 1 Amgen Center Dr, Mailstop 30E-2-C, Thousand Oaks, CA 91320 dekeyser@amgen.com

§JDK and EML contributed equally to this manuscript

Address Correspondence to: Curt Omiecinski PhD, 101 Life Sciences Bldg., Pennsylvania State University, University Park, PA 16802 (814) 863-1625, (814) 863-1696 fax; cjo10@psu.edu

Abstract

Phthalates and other endocrine-disruptive chemicals are manufactured in large quantities for use as plasticizers and other commercial applications, resulting in ubiquitous human exposure and thus, concern regarding their toxicity. Innate defense against small molecule exposures is controlled in large part by the constitutive androstane receptor (CAR) and the pregnane X receptor (PXR). The human CAR gene undergoes multiple alternative splicing events resulting in the CAR2 and CAR3 variant receptors. Recent studies from our laboratory show that CAR2 is potently and specifically activated by di(2-ethylhexyl) phthalate (DEHP). We hypothesized that alternative splicing is a mechanism for increasing CAR's functional diversity, broadening the human receptors' repertoire of response to environmental xenobiotics. In these studies, we examine the interaction of alternatively spliced CARs and PXR with a range of suspected endocrine disruptors, including phthalates, bis-phenol A (BPA), and 4-N-nonylphenol (NP). Transactivation and two-hybrid studies in COS-1 cells revealed differential selectivity of endocrine disrupting chemicals for the variant CAR and PXR. Ex vivo studies showed DEHP and Di-isononyl phthalate (DiNP) potently induced CYP2B6 and CYP3A4 expression in human hepatocytes. Mutation analysis of CAR2, *in silico* modeling, and ligand docking studies suggested that the SPTV amino acid insertion of CAR2 creates a unique ligand-binding pocket. Alternative gene splicing results in variant CAR receptors that selectively recognize phthalates and BPA. The interaction of phthalates with CAR and PXR suggests a xenobiotic response that is complex and biologically redundant.

Introduction

The innate defense against exposure to xenobiotics is controlled in large part by the expression of a milieu of metabolic enzymes and transporters. A critical part of this defense system is the xenobiotic exposure induced up-regulation of these enzymes and transporters, which is accomplished through transcriptional activation (Xu *et al.* 2005). Nuclear receptors play a vital role in this process. Nuclear receptors are superfamily of receptors that are ligand activated, and upon activation, bind to specific sequences proximal to target genes, resulting in increased gene expression. Two important members of this family are the constitutive androstane receptor (CAR) (Baes *et al.* 1994) and the pregnane X receptor (PXR) (Kliewer *et al.* 1998).

Together CAR and PXR orchestrate the expression of phase I, II and III metabolism enzymes (Wei *et al.* 2000; Wei *et al.* 2002) by heterodimerizing with the retinoid X receptor α (RXRα) and binding specific DNA response elements upstream of target genes. The battery of CAR target genes includes certain cytochrome P450s, UDP-glucuronosyltransferase, sulfotransferase, glutathione S-transferase, aldehyde dehydrogenase, and ABC transporter families (Maglich *et al.* 2002; Ueda *et al.* 2002). In addition to xenobiotics, CAR is also involved in regulation of metabolism of endogenous compounds such as bile acids (Guo *et al.* 2003) and steroid hormones (Xie *et al.* 2003). More recently, these receptors have been implicated in the regulation of liver energy metabolism (Kodama *et al.* 2004; Konno *et al.* 2008; Masson *et al.* 2008). CYP2B6 gene and CYP3A4 are the prototypical target genes for CAR (Sueyoshi *et al.* 1999) and PXR (Lehmann *et al.* 1998), respectively, but there is considerable cross-talk between the two receptors on the regulatory elements of these genes (Pascussi *et al.* 2003).

Our laboratory initially identified that alternative splicing events are important contributors to CAR expression (Auerbach *et al.* 2003), as corroborated by others (Jinno *et al.* 2004; Lamba *et al.* 2004a; Ross *et al.* 2010). Two prominent CAR splice variants are CAR2, generated by an

alternative splice acceptor site in intron 6, resulting in a 4 amino acid insertion (SPTV) in the vicinity of the receptor's ligand binding pocket, and CAR3, generated by an alternative splice acceptor site in intron 7, leading to a 5 amino acid insertion (APYLT) in the receptor's ligand binding/ heterodimerization domain (Auerbach *et al.* 2003). The CAR2 and CAR3 transcripts are prominently expressed in human liver and primary hepatocytes, with combined levels ranging up to ~50% of total CAR (Dekeyser *et al.* 2009; Jinno *et al.* 2004; Ross *et al.* 2010). Although immunologically indistinguishable with currently available antibody reagents, the variant receptor proteins are stable in *in vitro* expression systems, in bacteria, and in a host of transiently and stably-transfected mammalian cells (Auerbach *et al.* 2003; Chen *et al.* 2010; Dekeyser *et al.* 2009). While the reference human CAR (referred to hereafter as CAR1), has high constitutive activity in the absence of exogenous ligand, CAR2 and CAR3 require ligand for activity. The presence of multiple variants of CAR (Arnold *et al.* 2004; Jinno *et al.* 2004; Lamba *et al.* 2004b; Savkur *et al.* 2003), provides potential for increased diversity of the CAR gene. Notably, the CAR2 site is not conserved in marmoset, mouse, or rat, thus these species are incapable of generating a CAR2-like protein (Dekeyser *et al.* 2009).

Although controversial, phthalates, Bisphenol A, and nonylphenols are among the many chemicals that have been linked to endocrine disruption (Diamanti-Kandarakis *et al.* 2009). Because of their wide use in a variety of commercial and industrial applications, they are ubiquitous in the environment and the potential for human exposure is high (Bonefeld-Jorgensen *et al.* 2007; Schettler 2006). For example, in 2006 phthalate consumption reached 1,000,000 tons in Western Europe alone (Wittassek and Angerer 2008a). In a previous report, we demonstrated that di(2-ethylhexyl) phthalate (DEHP) is a highly potent agonist of CAR2, but is not a strong agonist of CAR1 or CAR3 (Dekeyser *et al.* 2009). This observation provided strong support for the hypothesis that alternative splicing of the CAR gene is a mechanism for increasing the functional diversity of the receptor. The current studies further examine phthalates and other EDC as activators of xenobiotic metabolism pathways through human

CAR variants and PXR, and to examine specific properties of CAR2 that allow for its high affinity binding to DEHP and DiNP.

Materials and Methods

Chemicals. Di(2-ethylhexyl) phthalate (DEHP, CAS #117-81-7), 5α-androstan-3α-ol (ANDRO, CAS #7657-50-3), Di-isononyl phthalate (DiNP, CAS #68515-48-0) and dimethyl sulfoxide (DMSO, CAS #67-68-5), Phenobarbital (PB, CAS #50-06-6) Bisphenol A (CAS #80-05-7) and Nonylphenol (CAS #104-40-5) were purchased from Sigma-Aldrich (St. Louis, MO). Diethyl phthalate (DEP, CAS #84-66-2), di-n-butyl phthalate (DnBP, CAS #84-74-2) and di-isobutyl phthalate (DiBP, CAS #84-69-5) were purchased from Alfa Aesar (Ward Hill, MA). 6-(4-Chlorophenyl)imidazo[2,1-b] [1,3]thiazole-5-carbaldehyde O-3,4-dichlorobenzyl) oxime (CITCO, CAS #338404-52-7) was obtained from BIOMOL Research Laboratories (Plymouth Meeting, PA). Rifampicin was purchased from VWR Biosciences. TO901317 (TO, CAS #293754-55-9) was obtained from Cayman Chemical Co. (Ann Arbor, MI). All compounds were >98% pure except DiNP, which is manufactured as mixture of 9 carbon isomers. Structures are shown in Figure 1.

Cell culture and transfections. Culture conditions for maintenance of COS-1 cells (ATCC, Manassas, VA) were previously published (Auerbach *et al.* 2005). COS-1 cells were used since they are devoid of endogenous CAR expression/activity as demonstrated in previous reports (Auerbach *et al.* 2005; Auerbach *et al.* 2007) and by the current study, as no CAR reporter activity is detected in COS-1 cells transfected with empty expression vectors. For transfection and chemical treatments, the same medium was used except dextran/charcoal treated FBS (HyClone, Logan, UT) replaced normal FBS. All transfections for luciferase reporter and mammalian two-hybrid assays were performed in a 48-well format. The vectors CMV2-CAR1, CMV2-CAR2, CMV-CAR2A, CMV-CAR2D, 3.1-RXRα, 2B6-XREM-PBREM luciferase reporter and 3A4-XREM-pER6 luciferase reporter were described previously (Auerbach *et al.* 2007). The

vector CMV2-CAR3 and mammalian two-hybrid vectors were also reported previously (Auerbach *et al.* 2005). Experimental treatments were performed in triplicate or quadruplicate, and all experiments were repeated at least once. Transfections for transactivation and mammalian two-hybrid assays were preformed as previously described (Auerbach *et al.* 2005), except in the two hybrid assays, equal amounts (20 ng) of the pM-CAR (Gal4 DNA binding domain) and VP16-SRC1 (activation domain) vectors were used. Since RXRα is CAR and PXRs' heterodimer partner, a 3.1-RXRα ligand biding domain vector was included in the mammalian two-hybrid assays. All test compounds were diluted in DMSO and levels never exceeded 0.2% (vol/vol). As positive controls, CITCO for CAR variants (Maglich *et al.* 2003); or RFPM (Bertilsson *et al.* 1998) or TO (Mitro *et al.* 2007) for PXR were included. Because CAR1 is constitutively active, ANDRO (10μM), a mouse CAR (Forman *et al.* 1998) and human CAR1 (Auerbach *et al.* 2007) inverse-agonist, was included to decrease its activity, which can be restored in the presence of an agonist. All chemical treatments were for 24 h and luciferase assays were performed as previously described (Dekeyser *et al.* 2009).

Human primary hepatocyte culture. Normal human hepatocytes were obtained through Dr. Stephen Strom from the Liver Tissue Cell Distribution System, Pittsburgh, PA, funded by NIH Contract #N01-DK-7-0004/HHSN267200700004C. Cell culture conditions were published previously (Goyak *et al.* 2008). The medium was replaced every 24 h. Hepatocytes were treated with vehicle control (0.1% DMSO), PB (1mM), CITCO (2μM), DEHP (0.1, 1, or 10μM) or DINP (0.1, 1, or 10μM) 72 h after the first medium change. After a 48 hr treatment, cells were harvested in 250μl of ice-cold cell lysis buffer (20mM Tris-HCl, pH 7.5 containing 100mM NaCl, 0.5% NP40 and 1X protease cocktail inhibitor) and incubated on ice for 30 min. The cell lysates were sonicated and centrifuged to collect supernatants. Total protein concentration was determined with the Pierce 660 Protein Assay using a Nanodrop 2000 spectrophotometer (Thermo Scientific).

Western blot analyses. Cell lysate supernatants (25 µg) from treated human primary hepatocytes were separated on 10% SDS-polyacrylamide gels, and electrophoretically transferred onto Immuno-Blot PVDF membranes (Bio-Rad). The membranes were blocked in 5% non-fat dry milk in 1X Tris-buffered saline containing 0.1% Tween-20 (0.1% TBST). The membranes were then incubated with specific antibodies against human CYP2B6 or CYP3A4 (obtained from Dr. Harry C. Gelboin, NIH), diluted 1:1000 in 2% non-fat dry milk in 0.1% TBST, respectively. β-actin (Santa Cruz, CA) was used as internal control. Blots were washed and incubated with horseradish peroxidase goat anti-mouse IgG antibody diluted 1:5000 in 2% non-fat dry milk in 0.1% TBST. Blots were developed using Pierce Super-signal ECL Western blotting detection reagents (Thermo Scientific).

Ligand binding domain modeling and ligand docking. The Phyre (Protein homology/analogy recognition engine) modeling program was used to generate CAR2 and CAR3 ligand binding domain models with the assistance of Dr. Lawrence Kelley (Kelley and Sternberg 2009). The quality of the models was assessed with RAMPAGE (http://mordred.bioc.cam.ac.uk/~rapper/rampage.php; (Lovell *et al.* 2003)). The structures of the ligand binding pocket (LBP) of the CAR1 structure (Xu *et al.* 2004) and the Phyre generated CAR2 and CAR3 models were then characterized using Pocket-Finder (http://bmbpcu36.leeds.ac.uk/pocketfinder/) (Laurie and Jackson 2005). ICM MolSoft Browser Pro (http://www.molsoft.com/) was used to visualize CAR and CAR3 predicted structures and CAR1 models and LBP.

For the docking simulations of DEHP into the Phyre CAR2 structural model, AutoDock4 (Morris *et al.* 2009) and AutoDock Vina (Trott and Olson 2010) were used with AutoDockTools graphical user interface. Prior to docking, all polar hydrogens were added to the molecules. The ligands were allowed to rotate freely around all active torsions during docking, while the protein structures remained rigid. A 22 x 22 x 22 Å grid box was used to center the docking algorithm on the ligand binding site. All other settings were defaults in AutoDock Vina. The resulting ligand

docking configurations were analyzed for lowest binding energy (kcal/mol) and visualized using and Molsoft Browser Pro.

Statistical Analysis. Statistics and EC_{50} values were obtained using GraphPad Prism 5 (GraphPad Software, San Diego, CA). For determining differences in activation of CAR or PXR by various treatments, two-way ANOVAs were performed, followed by a Bonferroni test for comparison to controls.

Results

BPA activates CAR1 and CAR3. Based on our previous finding that DEHP is a potent activator of CAR2, we examined the ability of BPA and NP, both plasticizers with reported estrogenic activity, to activate CAR variants and PXR. At 0.1 and 10 µM, BPA reactivated reporter activity through CAR1 to levels about equal to CITCO, while 10 µM BPA activated CAR3 to levels about 60% of CITCO-induced reactivation (Figure 2). BPA, even at the higher dose, showed no activation of the promoter through CAR2 and only a small effect on PXR. NP (0.1 and 10 µM) activated the 2B6-XREM-PBREM reporter through CAR1 to levels about 45% of CITCO-induced activation with no effect on CAR2, CAR3 or PXR.

CAR and PXR recognize a broad range of phthalates. We next examined the abilities of DEP, DnBP, DiBP and DiNP to activate the 2B6-XREM-PBREM reporter through CAR1, CAR2, CAR3, and PXR (Figure 3A-D). No activity was observed in cells transfected with the empty CMV2 vector (data not shown). For CAR1, 10 µM ANDRO was included in all treatments except DMSO. DEP showed little or no activation of the 2B6-XREM-PBREM reporter through any of the CAR variants or PXR, while DnNP and DiBP were weak activators of CAR1, CAR2, CAR3, and PXR. In contrast, DiNP displayed maximal activation of the 2B6-XREM-PBREM reporter (compared to CITCO) through CAR2 (Figure 3B), with no activation of CAR1 or CAR3. DiNP was a weak activator of PXR through the 2B6-XREM-PBREM reporter. We also tested

phthalate activation of the 3A4-XREM-pER6 reporter through PXR and the results were essentially identical to those with the 2B6-XREM-PBREM (Supplemental Figure S1).

The strong activation of CAR2 by DEHP and DiNP prompted us to directly compare these two phthalates in transactivation assays over a range of doses, and to confirm our results with CAR1, CAR3 and PXR (Figure 3E-3H). For CAR1 and CAR3, DEHP and DiNP showed little activation of the 2B6-XREM-PBREM reporter (Figure 3E and 3G). In contrast, DEHP and DiNP activated the reporter through CAR2 with a much higher affinity than CITCO. Furthermore, DEHP exhibited approximately 3X higher affinity than DiNP (Figure 3F). We used TO as a positive control for PXR, as it is much more potent than RFPM (Mitro *et al.* 2007); TO does not activate the CAR variants (Supplemental Figure S2). DEHP and DiNP both activated the 2B6- (Figure 3H) and 3A4-XREM-pER6 (Supplemental Figure S3) through PXR with equal affinity, however they were much less potent than TO. The EC_{50} values for activation of 2B6-XREM-PBREM each of the compounds tested with CAR2, CAR3 and PXR are shown in Table 1. For CAR1, EC_{50} values were not determined due to the inherent problem of its constitutive activity.

We also tested DEHP and DiNP activation of CAR and PXR using a mammalian two-hybrid protein interaction assay. Again, DEHP and DiNP showed very little or no activation of CAR1 or CAR3 (data not shown). DEHP and DiNP were both potent activators of CAR2 relative to CITCO, showing the same rank order potency as in the transactivation assay (Figure 4A). For PXR, DEHP and DiNP exhibited only moderate activity (Figure 4B). The doses of DEHP and DiNP required for maximal activation of the reporter through PXR were about 10-100X higher than were required for CAR2. These studies suggest DEHP and DiNP are potent activators of CAR2, with selectivity at lower concentrations for CAR2 over PXR.

DEHP and DiNP induce CYP2B6 and CYP3A4 protein in human hepatocytes. To support our *in vitro* findings, DEHP and DiNP treated human hepatocytes from four separate donors were assessed for CYP2B6 and CYP3A4 protein levels. A representative immunoblot from one donor is shown in Figure 5. CITCO (2 μM) and PB (1 mM) were positive controls. DEHP and

DiNP resulted in markedly increased CYP2B6 and CYP3A4 protein expression relative to DMSO controls. A dose response relationship was evident for CYP2B6 and CYP3A4 in the DiNP treated samples, but not in the DEHP treated samples. This result was similar for all of the donors except one, which exhibited increased CYP2B6 and CYP3A4 relative to DMSO controls, however, the increase was modest and did not exhibit a dose-response relationship for either protein.

Mutation of CAR2 greatly alters the response to DEHP and DiNP. To further evaluate the contribution of the CAR2 SPTV insertion DEHP and DiNP activity, two mutant constructs were tested in transactication assays. The serine 233, a polar uncharged residue, was replaced with either an alanine, a small hydrophobic uncharged residue (S233A, CAR2A), or aspartate, a larger, negatively charged residue (S233D, CAR2D) in order to determine how these differences affect DEHP and DiNP interaction with the CAR2 receptor. CITCO was also included as a reference. The CAR2 mutations had the least impact on CITCO EC_{50} (Figure 6A). The CAR2 and CAR2A mutant exhibited approximately equal EC_{50} for CITCO, while the CAR2D mutation resulted in a ~2X increase in EC_{50}. Although the CAR2A mutation appeared to reduce CITCO's E_{max}, the CAR2A and CAR2D mutations had a marked impact on the EC_{50} of DEHP and DiNP. The CAR2A mutant displayed a greatly reduced EC_{50} (~10X more potent) for DEHP and DiNP, in comparison to the endogenous CAR2 receptor (Figure 6B and C). The CAR2D substitution markedly decreased DEHP and DiNP activation; the DEHP EC_{50} value with CAR2D was ~10X higher than CAR2. An EC_{50} value for DiNP with CAR2D was not determined because the dose response curve was not complete, however, higher doses of DiNP are likely not physiologically relevant.

CAR2 model suggests altered LBP, relative to CAR1 and CAR3. The Phyre protein modeling program predicted CAR2 structure was superimposed on the CAR1 structure (1XVP) for comparison (Figure 7, panels A and B). Generally, the main chain coordinates of the CAR structures are very similar, with the exception of the amino acids flanking the SPTV CAR2

insertion. While the SPTV insertion (shown in yellow) aligns with the alpha helix of CAR1 (red), a region on the N-terminal side of the insertion forms an unstructured loop (green). Ramachandran analysis of CAR2 revealed that 94% of the residues were in favored regions, 4% were in allowed regions and 2% were in outlier regions. Notably, one outlier was the serine of the SPTV insertion, probably because as a pre-proline residue, the phi-psi bond angles were not favored.

Because of the proximity of the SPTV insertion to the CAR LBP and the differences in ligand specificity of CAR2, we submitted the CAR1 structure (1XVP) and the CAR2 Phyre model for LBP detection. Figure 7 (panel C) shows the superimposed CAR1 (red) and CAR2 (aqua) LBP representations generated by the PockerFinder algorithm with their respective ligands, CITCO (red) for CAR1, or DEHP (blue) for CAR2. Calculated pocket volumes for the CAR1 crystal structure and the Phyre CAR2 model were 722 and 662 $Å^3$, respectively. The CAR1 PocketFinder calculated volume was similar to the reported pocket volume of 675 $Å^3$ (Xu *et al.* 2004). Although the CAR1 and CAR2 predicted volumes were similar, the shapes of the pockets differed, as were the orientations of the respective ligands in the pockets (Figure 7C-E).

The CAR3 sequence was also submitted for structure prediction and subsequent pocket detection (data not shown). For the CAR3 model, Ramachandran analysis showed that 86.3% of the residues were in favored regions, 11.2% were in allowed regions and 2% were in outlier regions One outlier was an arginine (R277), which was also a pre-proline residue, two residues away from the carboxy-end of the APYLT insertion. The calculated pocket volume (701 $Å^3$) of CAR3 was virtually identical to pocket predicted for CAR1 (model not shown), an anticipated result since the APLYT insertion lies between helices 8 and 9, and therefore not expected to affect the LBP.

Discussion

The studies presented here provide novel insights into the CAR/PXR xenobiotic sensing systems and demonstrate that the variant CARs and PXR possess distinct ligand-selective activation profiles. Our previous observation that DEHP is a highly potent agonist of CAR2 (Dekeyser *et al.* 2009), coupled to our new findings, reveal that alternative splicing of CAR functions to enhance the receptors' ability to distinguish a broad range of xenobiotics that otherwise possess similar chemical properties. We also identify BPA as a CAR1 and CAR3 agonist, with little effect on CAR2 activation. The finding that CAR1 and CAR3 have similar ligand binding properties that are distinct from CAR2, supports the conceptual use of CAR3 as a tool for higher throughput prediction of CAR1 ligands, as suggested previously (Auerbach *et al.* 2005; Faucette *et al.* 2007). Further, the ability of phthalates to activate PXR, albeit at high concentrations relative to CAR2, provides insight into the crosstalk between the two receptors.

DEHP and DiNP induced expression of CYP2B6 and CYP3A4 proteins in primary human hepatocytes, however they were not as potent as CITCO, which contrasts our *in vitro* studies. This discrepancy may be due to the extensive hepatic metabolism of phthalates in humans (Frederiksen *et al.* 2007; Wittassek and Angerer 2008b). Nevertheless, induction is likely mediated *via* CAR2 at low exposure concentrations, and perhaps by both CAR2 and PXR at higher, e.g., 10 µM concentrations. While the induction response was relatively consistent among the donors, one donor exhibited lesser responsiveness. We previously observed interindividual variability in the hepatocyte induction of CYP2B6 and CYP3A4 mRNA by DEHP (Dekeyser *et al.* 2009), as well as to other prototypical inducers (Goyak *et al.* 2008). Differential xenobiotic responsiveness among humans likely results from a complex interplay of genetics, previous chemical exposures, and perhaps differences in the expression profiles of the xenobiotic receptors that mediate these responses.

It is noteworthy that DEHP- and DiNP-mediated induction of both CYP2B6 and CYP3A4 proteins was apparent even at the lowest concentration tested (100 nM). Data from our transcriptional transactivation experiments indicated that even lower DEHP concentrations, e.g.

10 nM, are capable of activating CAR2 (Figure 6B). Human studies have reported mean DEHP blood levels of 4.8 µM in humans undergoing dialysis (Pollack *et al.* 1985). Additionally, a study of Swedish mothers (Hogberg *et al.* 2008) found significant levels of DEHP in serum (median 1.2 nM, mean 15 nM) and maternal milk (mean 43 nM). Thus, vulnerable populations appear exposed to DEHP at concentrations that likely activate CAR2 and/or PXR. DEHP and DiNP are extensively metabolized and based on urinary excretion of DEHP and DiNP metabolites, even 'normal, healthy' humans are likely exposed to low but significant levels of DEHP and DiNP (Meeker *et al.* 2009; Silva *et al.* 2006), levels that may activate CAR2. Further, Silva et al. suggest that human DiNP exposures may be underestimated, since DiNP is an isomeric mixture that is extensively metabolized and only a few metabolites are measured when assessing human exposures (Silva *et al.* 2006). While DEHP appears more potent than DiNP by measures of both CYP450 induction and transcriptional transactivation activity, it should be noted that as a mixture of 9-carbon isomers, it is possible that only select DiNP isomers contribute to the activation responses noted. This aspect will require further study; however, it is likely that most human exposures are to DiNP isomer mixtures.

Although we did not test BPA in hepatocytes, our transactivation assays demonstrated that BPA activated CAR1 and CAR3 at concentrations of 10 µM. To our knowledge, this is the first report of BPA activation of human CAR variants. However, the EC_{50} of BPA for estrogenic activity in MCF-7 cells is 0.63 µM (Kitamura *et al.* 2005). In addition, BPA also mediates other pathways that do not involve nuclear receptors at subnanomolar doses (Welshons *et al.* 2006); thus, our prediction is that CAR is not involved in BPA-induced effects at lower doses. Another interesting observation was that NP had little or no activity with human CAR variants or human PXR. These latter results are in contrast to a report that NP activates mouse and human CAR and human PXR (Hernandez *et al.* 2007). The differences noted may result from the NP preparations used. Our study used a 99% pure preparation of 4-N-NP, whereas the Hernandez study used technical grade 4-NP, which is an 85% para-isomer mix (Hernandez *et al.* 2007).

We performed mutagenesis studies to investigate potential mechanisms of how CAR2's SPTV insertion contributes to ligand specificity. Mutation of the S233 residue greatly alters the receptor's response to DEHP and DiNP. Replacing S233 with the smaller, more hydrophobic alanine residue (CAR2A) may have created a more hydrophobic LBP environment for interacting with the alkyl chains of DEHP and DiNP, and thus, increased the response to these compounds. In contrast, substitution of S233 with aspartic acid, which has a slightly larger volume than serine and is negatively charged, may have created a less favorable LBP environment for DEHP and DiNP, resulting in a markedly decreased response. The differences in DEHP and DiNP response among the CAR2 mutants were not nearly as pronounced with the pan-CAR ligand, CITCO. Taken together, these results suggest that the naturally occurring SPTV insertion of CAR2 alters the nature of the receptor's LBP and creates a more favorable binding site conformation for DEHP and DiNP.

The differences in activation of the CAR variants by phthalates and BPA are important observations regarding the diversity of CAR, and led us to further investigate the nature of the CAR LBP using CAR2 and CAR3 structural models. The human CAR1 ligand binding domain has been characterized in the presence of two agonists, CITCO and 5β-preganedione (Xu *et al.* 2004). These studies show that helices 2, 3, 4, 5, 6, 7 and 10 and β-strands 3 and 4 surround the LBP of CAR1. Further, amino acids in helix 3, 5, 6 and 7 are important for ligand binding. The SPTV insertion between helix 6 and 7 thus likely alters the spatial orientation of this region, resulting in altered ligand specificity. Although the overall volume of the modeled CAR2 LBP was similar, the results suggested that the CAR2 SPTV leads to an altered LBP conformation in comparison to CAR1 and CAR3. Specifically, the CAR2 insertion is predicted to alter the conformation of helix 6, allowing for an expanded pocket proximal to that region.

In silico comparisons of CITCO in the CAR1 structure with that of docked DEHP within the CAR2 pocket suggests these compounds exploit respective differences of their chemistries, as well as their LBP. DEHP is primarily a hydrophobic molecule that appears to interact with CAR2

through hydrophobic interactions. One alkyl side-chain of DEHP appears to project into the expanded region of the CAR2 pocket, which is primarily bounded by hydrophobic amino acids F217, I226, and F247. In the CAR1 structure, the CITCO imidazothiazole moiety extends into a more polar region of the pocket, enclosed by N165, C202, H203, and Y326 (Xu *et al.* 2004). In the CAR2 predicted pocket, DEHP does not appear to utilize this portion of the LBP. Although the LBPs are displayed to emphasize the differences (Figure 7C-E), an interesting similarity is that the phenyl ring of DEHP is almost superimposed with the para-chlorophenyl ring of CITCO (not shown), lending enhanced credibility to the modeling predictions. However, efforts are required and ongoing to obtain the actual crystal structure of CAR2.

Initial concerns regarding phthalates focused on peroxisome proliferation demonstrated in rodents through PPAR activation; concerns that have since waned as humans are relatively refractory to peroxisome proliferation (Rusyn *et al.* 2006). More recently, concern has shifted towards possible anti-androgenic endocrine disrupting effects of phthalates (Kavlock *et al.* 2006). It is well established that both CYP2B6 and CYP3A4 are induced by CAR and PXR and that these enzymes are involved in testosterone metabolism (Imaoka *et al.* 1996). The potential impact of phthalates on androgen metabolism through the activation of CAR and PXR will require additional investigation. Further, the emerging regulatory role of CAR in energy metabolism and insulin sensitivity (Dong *et al.* 2009; Gao *et al.* 2009; Konno *et al.* 2008) also suggest intriguing areas for future phthalate research.

In comparison to the essentially infinite number of small molecules to which humans are exposed, the number of xenosensing receptors is relatively small. The current report demonstrates that alternatively spliced human *CAR* gene transcripts increase CAR's capacity to serve as a selective xenosensor. While mRNA for these splice variants has been detected as substantial levels in human liver (Dekeyser *et al.* 2009; Jinno *et al.* 2004; Ross *et al.* 2010), it is noteworthy that most rodent species, due to the absence of a canonical splice acceptor site, appear incapable of producing the CAR2 variant. These differences, when combined with the

known species differences in the receptors' ligand specificity, suggest that rodent models alone may not be adequate for the study of human CAR activation responses (Dekeyser *et al.* 2009). Finally, the observation that phthalates extensively interact with the human CAR and PXR receptors, and that CAR2 is extraordinarily sensitive to both DEHP and DiNP, provides new direction for investigating the toxicological implications of human exposure to these ubiquitous environmental agents.

Funding Information

This work was supported by NIH Grant R01 GM066411 (CJO).

Acknowledgments

The authors would like to express special thanks to Dr. Stephen Strom for his support and assistance with human hepatocyte procurement.

References

Arnold, K. A., Eichelbaum, M., and Burk, O. (2004). Alternative splicing affects the function and tissue-specific expression of the human constitutive androstane receptor. *Nucl. Recept.* **2**(1), 1.

Auerbach, S. S., Dekeyser, J. G., Stoner, M. A., and Omiecinski, C. J. (2007). CAR2 displays unique ligand binding and RXRalpha heterodimerization characteristics. *Drug Metab Dispos.* **35**(3), 428-439.

Auerbach, S. S., Ramsden, R., Stoner, M. A., Verlinde, C., Hassett, C., and Omiecinski, C. J. (2003). Alternatively spliced isoforms of the human constitutive androstane receptor. *Nucleic Acids Res.* **31**(12), 3194-3207.

Auerbach, S. S., Stoner, M. A., Su, S., and Omiecinski, C. J. (2005). Retinoid X Receptor-{alpha}-Dependent Transactivation by a Naturally Occurring Structural Variant of Human Constitutive Androstane Receptor (NR1I3). *Mol. Pharmacol.* **68**(5), 1239-1253.

Baes, M., Gulick, T., Choi, H. S., Martinoli, M. G., Simha, D., and Moore, D. D. (1994). A new orphan member of the nuclear hormone receptor superfamily that interacts with a subset of retinoic acid response elements. *Mol. Cell Biol.* **14**(3), 1544-1551.

Bertilsson, G., Heidrich, J., Svensson, K., Asman, M., Jendeberg, L., Sydow-Backman, M., Ohlsson, R., Postlind, H., Blomquist, P., and Berkenstam, A. (1998). Identification of a human nuclear receptor defines a new signaling pathway for CYP3A induction. *Proc. Natl. Acad. Sci. U. S. A* **95**(21), 12208-12213.

Bonefeld-Jorgensen, E. C., Long, M., Hofmeister, M. V., and Vinggaard, A. M. (2007). Endocrine-disrupting potential of bisphenol A, bisphenol A dimethacrylate, 4-n-nonylphenol, and 4-n-octylphenol in vitro: new data and a brief review. *Environ. Health Perspect.* **115 Suppl 1**, 69-76.

Chen, T., Tompkins, L. M., Li, L., Li, H., Kim, G., Zheng, Y., and Wang, H. (2010). A single amino acid controls the functional switch of human constitutive androstane receptor (CAR) 1 to the xenobiotic-sensitive splicing variant CAR3. *J. Pharmacol. Exp. Ther.* **332**(1), 106-115.

Dekeyser, J. G., Stagliano, M. C., Auerbach, S. S., Prabu, K. S., Jones, A. D., and Omiecinski, C. J. (2009). Di(2-ethylhexyl) phthalate is a highly potent agonist for the human constitutive androstane receptor splice variant, CAR2. *Mol. Pharmacol.*

Diamanti-Kandarakis, E., Bourguignon, J. P., Giudice, L. C., Hauser, R., Prins, G. S., Soto, A. M., Zoeller, R. T., and Gore, A. C. (2009). Endocrine-disrupting chemicals: an Endocrine Society scientific statement. *Endocr. Rev.* **30**(4), 293-342.

Dong, B., Saha, P. K., Huang, W., Chen, W., Abu-Elheiga, L. A., Wakil, S. J., Stevens, R. D., Ilkayeva, O., Newgard, C. B., Chan, L., and Moore, D. D. (2009). Activation of

nuclear receptor CAR ameliorates diabetes and fatty liver disease. *Proc. Natl. Acad. Sci. U. S. A* **106**(44), 18831-18836.

Faucette, S. R., Zhang, T. C., Moore, R., Sueyoshi, T., Omiecinski, C. J., LeCluyse, E. L., Negishi, M., and Wang, H. (2007). Relative activation of human pregnane X receptor versus constitutive androstane receptor defines distinct classes of CYP2B6 and CYP3A4 inducers. *J. Pharmacol. Exp. Ther.* **320**(1), 72-80.

Forman, B. M., Tzameli, I., Choi, H. S., Chen, J., Simha, D., Seol, W., Evans, R. M., and Moore, D. D. (1998). Androstane metabolites bind to and deactivate the nuclear receptor CAR- beta. *Nature* **395**(6702), 612-615.

Frederiksen, H., Skakkebaek, N. E., and Andersson, A. M. (2007). Metabolism of phthalates in humans. *Mol. Nutr. Food Res.* **51**(7), 899-911.

Gao, J., He, J., Zhai, Y., Wada, T., and Xie, W. (2009). The constitutive androstane receptor is an anti-obesity nuclear receptor that improves insulin sensitivity. *J. Biol. Chem.* **284**(38), 25984-25992.

Goyak, K. M., Johnson, M. C., Strom, S. C., and Omiecinski, C. J. (2008). Expression profiling of interindividual variability following xenobiotic exposures in primary human hepatocyte cultures. *Toxicol. Appl. Pharmacol.* **231**(2), 216-224.

Guo, G. L., Lambert, G., Negishi, M., Ward, J. M., Brewer, H. B., Jr., Kliewer, S. A., Gonzalez, F. J., and Sinal, C. J. (2003). Complementary roles of farnesoid X receptor, pregnane X receptor, and constitutive androstane receptor in protection against bile acid toxicity. *J. Biol. Chem.* **278**(46), 45062-45071.

Hernandez, J. P., Huang, W., Chapman, L. M., Chua, S., Moore, D. D., and Baldwin, W. S. (2007). The environmental estrogen, nonylphenol, activates the constitutive androstane receptor. *Toxicol. Sci.* **98**(2), 416-426.

Hogberg, J., Hanberg, A., Berglund, M., Skerfving, S., Remberger, M., Calafat, A. M., Filipsson, A. F., Jansson, B., Johansson, N., Appelgren, M., and Hakansson, H. (2008). Phthalate diesters and their metabolites in human breast milk, blood or serum, and urine as biomarkers of exposure in vulnerable populations. *Environ. Health Perspect.* **116**(3), 334-339.

Imaoka, S., Yamada, T., Hiroi, T., Hayashi, K., Sakaki, T., Yabusaki, Y., and Funae, Y. (1996). Multiple forms of human P450 expressed in Saccharomyces cerevisiae. Systematic characterization and comparison with those of the rat. *Biochem. Pharmacol.* **51**(8), 1041-1050.

Jinno, H., Tanaka-Kagawa, T., Hanioka, N., Ishida, S., Saeki, M., Soyama, A., Itoda, M., Nishimura, T., Saito, Y., Ozawa, S., Ando, M., and Sawada, J. (2004). Identification of novel alternative splice variants of human constitutive androstane receptor and characterization of their expression in the liver. *Mol. Pharmacol.* **65**(3), 496-502.

Kavlock, R., Barr, D., Boekelheide, K., Breslin, W., Breysse, P., Chapin, R., Gaido, K., Hodgson, E., Marcus, M., Shea, K., and Williams, P. (2006). NTP-CERHR Expert Panel Update on the Reproductive and Developmental Toxicity of di(2-ethylhexyl) phthalate. *Reprod. Toxicol.* **22**(3), 291-399.

Kelley, L. A., and Sternberg, M. J. (2009). Protein structure prediction on the Web: a case study using the Phyre server. *Nat. Protoc.* **4**(3), 363-371.

Kitamura, S., Suzuki, T., Sanoh, S., Kohta, R., Jinno, N., Sugihara, K., Yoshihara, S., Fujimoto, N., Watanabe, H., and Ohta, S. (2005). Comparative study of the endocrine-disrupting activity of bisphenol A and 19 related compounds. *Toxicol. Sci.* **84**(2), 249-259.

Kliewer, S. A., Moore, J. T., Wade, L., Staudinger, J. L., Watson, M. A., Jones, S. A., McKee, D. D., Oliver, B. B., Willson, T. M., Zetterstrom, R. H., Perlmann, T., and Lehmann, J. M. (1998). An orphan nuclear receptor activated by pregnanes defines a novel steroid signaling pathway. *Cell* **92**(1), 73-82.

Kodama, S., Koike, C., Negishi, M., and Yamamoto, Y. (2004). Nuclear receptors CAR and PXR cross talk with FOXO1 to regulate genes that encode drug-metabolizing and gluconeogenic enzymes. *Mol. Cell Biol.* **24**(18), 7931-7940.

Konno, Y., Negishi, M., and Kodama, S. (2008). The roles of nuclear receptors CAR and PXR in hepatic energy metabolism. *Drug Metab Pharmacokinet.* **23**(1), 8-13.

Lamba, J. K., Lamba, V., Yasuda, K., Lin, Y. S., Assem, M., Thompson, E., Strom, S., and Schuetz, E. (2004a). Expression of constitutive androstane receptor splice variants in human tissues and their functional consequences. *J Pharmacol. Exp. Ther.* **311**(2), 811-821.

Lamba, J. K., Lamba, V., Yasuda, K., Lin, Y. S., Assem, M., Thompson, E., Strom, S., and Schuetz, E. G. (2004b). Expression of CAR splice variants in human tissues and their functional consequences. *J. Pharmacol. Exp. Ther.* **311**, 811-821.

Laurie, A. T., and Jackson, R. M. (2005). Q-SiteFinder: an energy-based method for the prediction of protein-ligand binding sites. *Bioinformatics.* **21**(9), 1908-1916.

Lehmann, J. M., McKee, D. D., Watson, M. A., Willson, T. M., Moore, J. T., and Kliewer, S. A. (1998). The human orphan nuclear receptor PXR is activated by compounds that regulate CYP3A4 gene expression and cause drug interactions. *J. Clin. Invest* **102**(5), 1016-1023.

Lovell, S. C., Davis, I. W., Arendall, W. B., III, de Bakker, P. I., Word, J. M., Prisant, M. G., Richardson, J. S., and Richardson, D. C. (2003). Structure validation by Calpha geometry: phi,psi and Cbeta deviation. *Proteins* **50**(3), 437-450.

Maglich, J. M., Parks, D. J., Moore, L. B., Collins, J. L., Goodwin, B., Billin, A. N., Stoltz, C. A., Kliewer, S. A., Lambert, M. H., Willson, T. M., and Moore, J. T. (2003).

Identification of a novel human constitutive androstane receptor (CAR) agonist and its use in the identification of CAR target genes. *J. Biol. Chem.* **278**(19), 17277-17283.

Maglich, J. M., Stoltz, C. M., Goodwin, B., Hawkins-Brown, D., Moore, J. T., and Kliewer, S. A. (2002). Nuclear pregnane x receptor and constitutive androstane receptor regulate overlapping but distinct sets of genes involved in xenobiotic detoxification. *Mol. Pharmacol.* **62**(3), 638-646.

Masson, D., Qatanani, M., Sberna, A. L., Xiao, R., Pais de Barros, J. P., Grober, J., Deckert, V., Athias, A., Gambert, P., Lagrost, L., Moore, D. D., and Assem, M. (2008). Activation of the constitutive androstane receptor decreases HDL in wild-type and human apoA-I transgenic mice. *J. Lipid Res.*

Meeker, J. D., Calafat, A. M., and Hauser, R. (2009). Urinary metabolites of di(2-ethylhexyl) phthalate are associated with decreased steroid hormone levels in adult men. *J. Androl* **30**(3), 287-297.

Mitro, N., Vargas, L., Romeo, R., Koder, A., and Saez, E. (2007). T0901317 is a potent PXR ligand: implications for the biology ascribed to LXR. *FEBS Lett.* **581**(9), 1721-1726.

Morris, G. M., Huey, R., Lindstrom, W., Sanner, M. F., Belew, R. K., Goodsell, D. S., and Olson, A. J. (2009). AutoDock4 and AutoDockTools4: Automated docking with selective receptor flexibility. *J. Comput. Chem.* **30**(16), 2785-2791.

Pascussi, J. M., Gerbal-Chaloin, S., Drocourt, L., Maurel, P., and Vilarem, M. J. (2003). The expression of CYP2B6, CYP2C9 and CYP3A4 genes: a tangle of networks of nuclear and steroid receptors. *Biochim. Biophys. Acta* **1619**(3), 243-253.

Pollack, G. M., Buchanan, J. F., Slaughter, R. L., Kohli, R. K., and Shen, D. D. (1985). Circulating concentrations of di(2-ethylhexyl) phthalate and its de-esterified phthalic acid products following plasticizer exposure in patients receiving hemodialysis. *Toxicol. Appl. Pharmacol.* **79**(2), 257-267.

Ross, J., Plummer, S. M., Rode, A., Scheer, N., Bower, C. C., Vogel, O., Henderson, C. J., Wolf, C. R., and Elcombe, C. R. (2010). Human constitutive androstane receptor (CAR) and pregnane X receptor (PXR) support the hypertrophic but not the hyperplastic response to the murine nongenotoxic hepatocarcinogens phenobarbital and chlordane in vivo. *Toxicol. Sci.* **116**(2), 452-466.

Rusyn, I., Peters, J. M., and Cunningham, M. L. (2006). Modes of action and species-specific effects of di-(2-ethylhexyl)phthalate in the liver. *Crit Rev. Toxicol.* **36**(5), 459-479.

Savkur, R. S., Wu, Y., Bramlett, K. S., Wang, M., Yao, S., Perkins, D., Totten, M., Searfoss, G., III, Ryan, T. P., Su, E. W., and Burris, T. P. (2003). Alternative splicing within the ligand binding domain of the human constitutive androstane receptor. *Mol. Genet. Metab* **80**(1-2), 216-226.

Schettler, T. (2006). Human exposure to phthalates via consumer products. *Int. J. Androl* **29**(1), 134-139.

Silva, M. J., Reidy, J. A., Preau, J. L., Jr., Needham, L. L., and Calafat, A. M. (2006). Oxidative metabolites of diisononyl phthalate as biomarkers for human exposure assessment. *Environ. Health Perspect.* **114**(8), 1158-1161.

Sueyoshi, T., Kawamoto, T., Zelko, I., Honkakoski, P., and Negishi, M. (1999). The repressed nuclear receptor CAR responds to phenobarbital in activating the human CYP2B6 gene. *J. Biol. Chem.* **274**(10), 6043-6046.

Trott, O., and Olson, A. J. (2010). AutoDock Vina: improving the speed and accuracy of docking with a new scoring function, efficient optimization, and multithreading. *J. Comput. Chem.* **31**(2), 455-461.

Ueda, A., Hamadeh, H. K., Webb, H. K., Yamamoto, Y., Sueyoshi, T., Afshari, C. A., Lehmann, J. M., and Negishi, M. (2002). Diverse roles of the nuclear orphan receptor CAR in regulating hepatic genes in response to phenobarbital. *Mol. Pharmacol.* **61**(1), 1-6.

Wei, P., Zhang, J., Dowhan, D. H., Han, Y., and Moore, D. D. (2002). Specific and overlapping functions of the nuclear hormone receptors CAR and PXR in xenobiotic response. *Pharmacogenomics. J.* **2**(2), 117-126.

Wei, P., Zhang, J., Egan-Hafley, M., Liang, S., and Moore, D. D. (2000). The nuclear receptor CAR mediates specific xenobiotic induction of drug metabolism. *Nature* **407**(6806), 920-923.

Welshons, W. V., Nagel, S. C., and vom Saal, F. S. (2006). Large effects from small exposures. III. Endocrine mechanisms mediating effects of bisphenol A at levels of human exposure. *Endocrinology* **147**(6 Suppl), S56-S69.

Wittassek, M., and Angerer, J. (2008a). Phthalates: metabolism and exposure. *Int. J. Androl* **31**(2), 131-138.

Wittassek, M., and Angerer, J. (2008b). Phthalates: metabolism and exposure. *Int. J. Androl* **31**(2), 131-138.

Xie, W., Yeuh, M. F., Radominska-Pandya, A., Saini, S. P., Negishi, Y., Bottroff, B. S., Cabrera, G. Y., Tukey, R. H., and Evans, R. M. (2003). Control of steroid, heme, and carcinogen metabolism by nuclear pregnane X receptor and constitutive androstane receptor. *Proc. Natl. Acad. Sci. U. S. A* **100**(7), 4150-4155.

Xu, C., Li, C. Y., and Kong, A. N. (2005). Induction of phase I, II and III drug metabolism/transport by xenobiotics. *Arch. Pharm. Res.* **28**(3), 249-268.

Xu, R. X., Lambert, M. H., Wisely, B. B., Warren, E. N., Weinert, E. E., Waitt, G. M., Williams, J. D., Collins, J. L., Moore, L. B., Willson, T. M., and Moore, J. T. (2004). A

structural basis for constitutive activity in the human CAR/RXRalpha heterodimer. *Mol. Cell* **16**(6), 919-928.

Table 1. Estimated EC_{50} values for activation of 2B6-XREM-PBREM through CAR2, CAR3 and PXR[a].

Ligand	CAR2	CAR3	PXR
DEP	NA[b]	267.6[c]	495.6
DnBP	24.1	8.0	12.5
DiBP	17.1	11.4	9.9
DiNP	0.34	NA	3.6
DEHP	0.1	NA	3.8
CITCO	0.9	0.1	ND[d]
Rifampicin	ND	ND	2.1
TO901317	NA	NA	0.03

[a]Not determined for CAR1 due to constitutive activation
[b]No or minimal activation
[c]All values are μM
[d]Not determined

Figure Legends

Figure 1. Structures of the compounds used in this study. All compounds were supplied at >98% purity and were isomerically pure, except DiNP, which was a mixture of 9 carbon isomers.

Figure 2. Activation of the 2B6-XREM-PBREM reporter by CAR1, CAR2 CAR3 or PXR after treatment with bis-phenol A or nonylphenol. Results shown here represent a single transfection experiment, with all treatments in quadruplicate. COS-1 cells were transfected with the 3.1-RXRα expression vector, the 2B6-XREM-PBREM reporter, the pRL-CMV vector for normalization of transfection efficiency and either CMV2-CAR1, CMV2-CAR2, CMV2-CAR3 or CMVs-PXR). All treatments were for 24h and the data are represented as normalized luciferase values and each data point represents the mean (+/- S.E.M.). *p<0.05 compared with androstanol control; **p<0.05 compared with DMSO control

Figure 3. Activation of the 2B6-XREM-PBREM reporter by CAR1, CAR2, CAR3 and PXR after treatment with phthalates. Results shown here represent a single transfection experiment, with all treatments in quadruplicate. COS-1 cells were transfected with 3.1-RXRα expression vector, the 2B6-XREM-PBREM reporter, the pRL-CMV vector for normalization of transfection efficiency and either CMV2-CAR1 (A, E), CMV2-CAR2 (B,F), CMV2-CAR3 (C,G) or CMV2-PXR (D,H). Panels A, B, C, and D show activity of various phthalates with each of the receptors. Panels E, F, G, and H show a more complete dose-response curve comparing DEHP, DiNP and the positive control CITCO for CAR1, CAR2 and CAR3 or TO901317 for PXR. All treatments were for 24h and the data are represented as normalized luciferase values and each data point represents the mean (+/- S.E.M.). *p<0.05 compared with androstanol control for CAR1 or DMSO control for CAR2, CAR3 and PXR.

Figure 4**.** DEHP and DiNP demonstrate selectivity for CAR2 in mammalian-two hybrid assay. COS-1 cells were transfected with CAR or PXR in the pm (GAL4) vector, SRC1 in the VP16 vector, 3.1 RXRα-LBD, pFR-luciferase reporter and pRL-CMV vector for normalization. Chemical treatments were for 24 h. Data are represented as normalized luciferase values and each data point represents the mean (+/- S.E.M.) of quadruplicate treatment wells from a representative transfection experiment.

Figure 5. Representative immunoblot showing expression of CYP2B6 and CYP3A4 in human hepatocytes treated with DEHP or DiNP. Human hepatocytes were treated with varying concentrations of DEHP and DiNP with DMSO, PB, and CITCO as controls for 48 h. Protein (S9 fractions) were isolated from lysed cells and subjected to immunoblot analysis with CYP2B6 or CYP3A4-specific antibodies. Actin is shown for normalization of protein loading.

Figure 6. Activation of the 2B6-XREM-PBREM reporter by CAR2, CAR2A, and CAR2D in response to CITCO, DEHP and DiNP. All transfections included the 3.1-RXRα expression vector, the 2B6-XREM-PBREM reporter, the pRL-CMV vector for normalization of transfection efficiency and either CMV2-CAR2 or CMV2-CAR2A. Cells were treated for 24 h. Data are represented as normalized luciferase values and each data point represents the mean (+/- S.E.M.) of quadruplicate treatment wells from a representative transfection experiment.

Figure 7. CAR2 predicted protein structure and CAR1 and CAR2 ligand binding pocket models. Panels A and B show two views the Phyre homology model of the human CAR2 receptor ligand binding domain (aqua) superimposed on the CAR1 ligand binding domain structure (red). CITCO (blue) is shown in the ligand binding pocket of CAR1. The CAR2 SPTV insertion is shown in yellow and a region adjacent to the insertion where the structure deviates from CAR1 is shown in green. Panel C shows an overlay of PocketFinder computer generated models of

the CAR1 (red) and CAR2 (aqua) LBP with their respective ligands, CITCO (red) and DEHP (blue). Panel D and E show the individual CAR1 and CAR2 LBP.

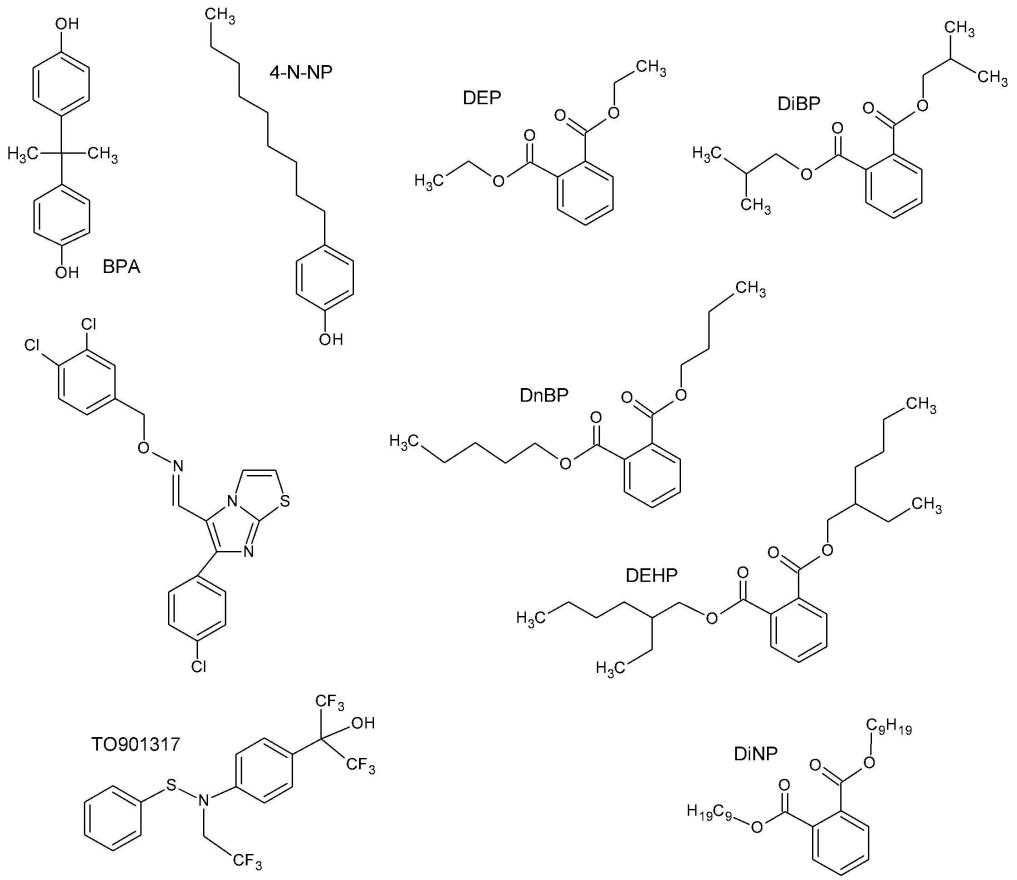

Figure 1. Structures of the compounds used in this study. All compounds were supplied at >98% purity and were isomerically pure, except DiNP, which was a mixture of 9 carbon isomers.

186x163mm (600 x 600 DPI)

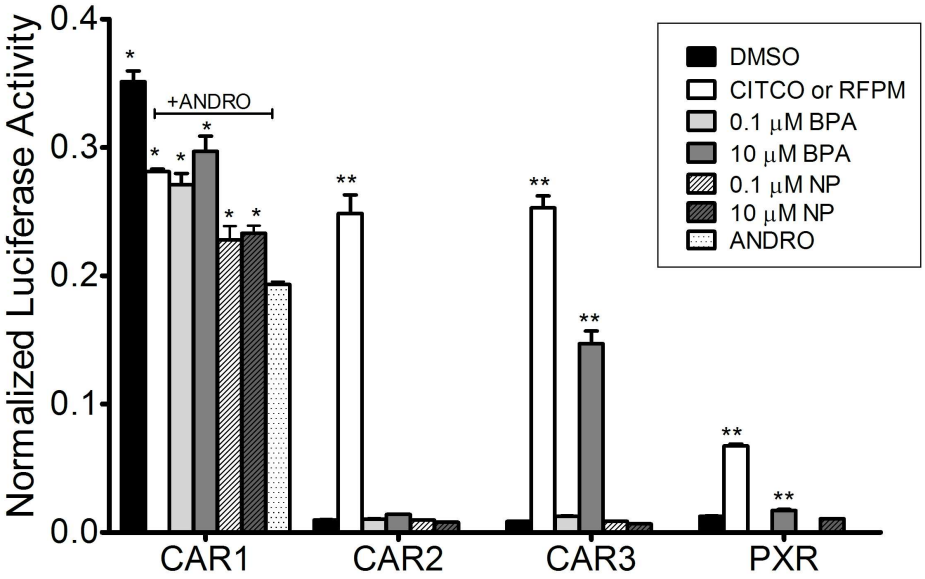

Figure 2. Activation of the 2B6-XREM-PBREM reporter by CAR1, CAR2 CAR3 or PXR after treatment with bis-phenol A or nonylphenol. Results shown here represent a single transfection experiment, with all treatments in quadruplicate. COS-1 cells were transfected with the 3.1-RXRα expression vector, the 2B6-XREM-PBREM reporter, the pRL-CMV vector for normalization of transfection efficiency and either CMV2-CAR1, CMV2-CAR2, CMV2-CAR3 or CMVs-PXR). All treatments were for 24h and the data are represented as normalized luciferase values and each data point represents the mean (+/- S.E.M.). *p<0.05 compared with androstanol control; **p<0.05 compared with DMSO control
205x129mm (300 x 300 DPI)

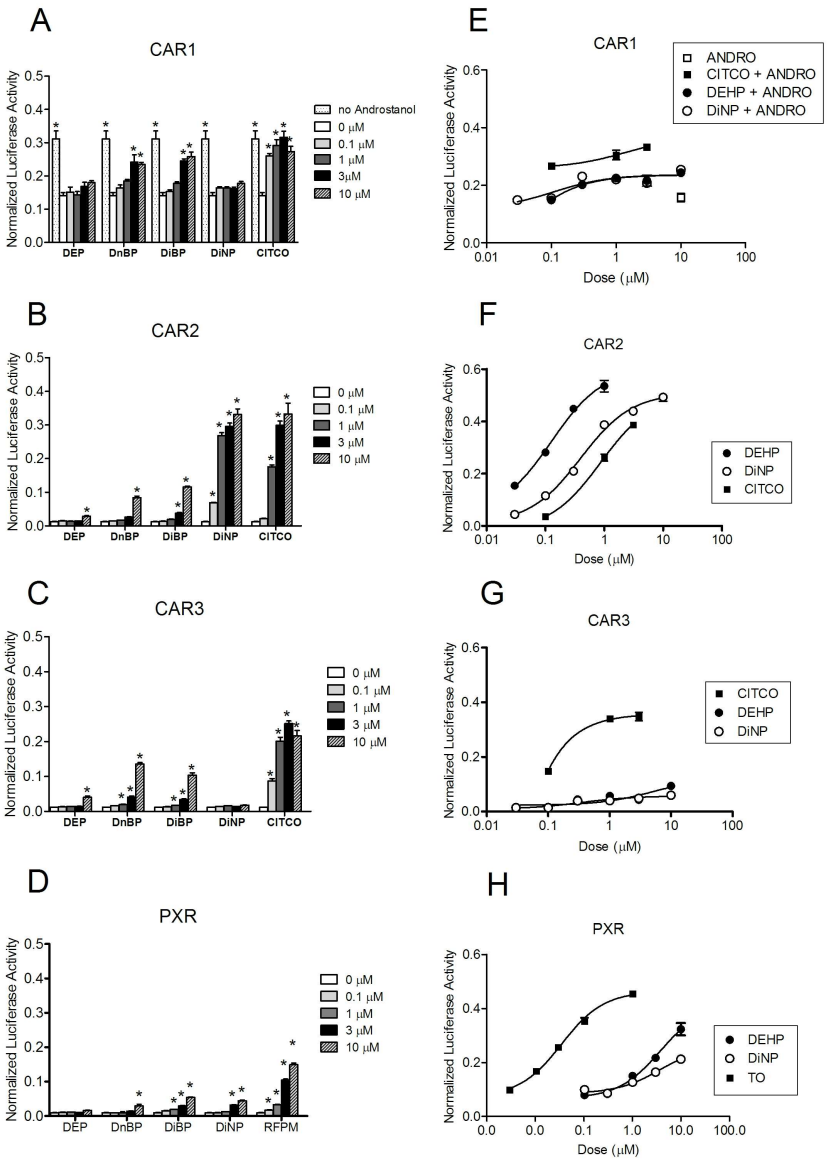

Figure 3. Activation of the 2B6-XREM-PBREM reporter by CAR1, CAR2, CAR3 and PXR after treatment with phthalates. Results shown here represent a single transfection experiment, with all treatments in quadruplicate. COS-1 cells were transfected with 3.1-RXRα expression vector, the 2B6-XREM-PBREM reporter, the pRL-CMV vector for normalization of transfection efficiency and either CMV2-CAR1 (A, E), CMV2-CAR2 (B,F), CMV2-CAR3 (C,G) or CMV2-PXR (D,H). Panels A, B, C, and D show activity of various phthalates with each of the receptors. Panels E, F, G, and H show a more complete dose-response curve comparing DEHP, DiNP and the positive control CITCO for CAR1, CAR2 and CAR3 or TO901317 for PXR. All treatments were for 24h and the data are represented as normalized luciferase values and each data point represents the mean (+/- S.E.M.). *p<0.05 compared with androstanol control for CAR1 or DMSO control for CAR2, CAR3 and PXR. 191x263mm (300 x 300 DPI)

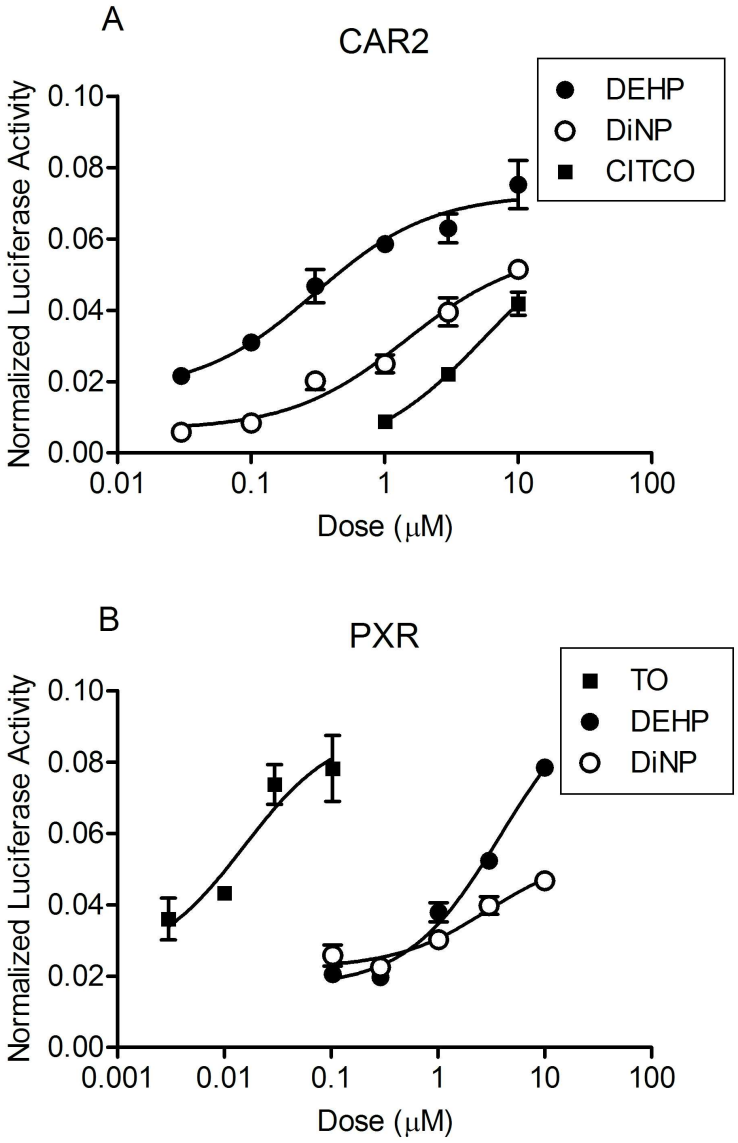

Figure 4. DEHP and DiNP demonstrate selectivity for CAR2 in mammalian-two hybrid assay. COS-1 cells were transfected with CAR or PXR in the pm (GAL4) vector, SRC1 in the VP16 vector, 3.1 RXRα-LBD, pFR-luciferase reporter and pRL-CMV vector for normalization. Chemical treatments were for 24 h. Data are represented as normalized luciferase values and each data point represents the mean (+/- S.E.M.) of quadruplicate treatment wells from a representative transfection experiment.
169x250mm (300 x 300 DPI)

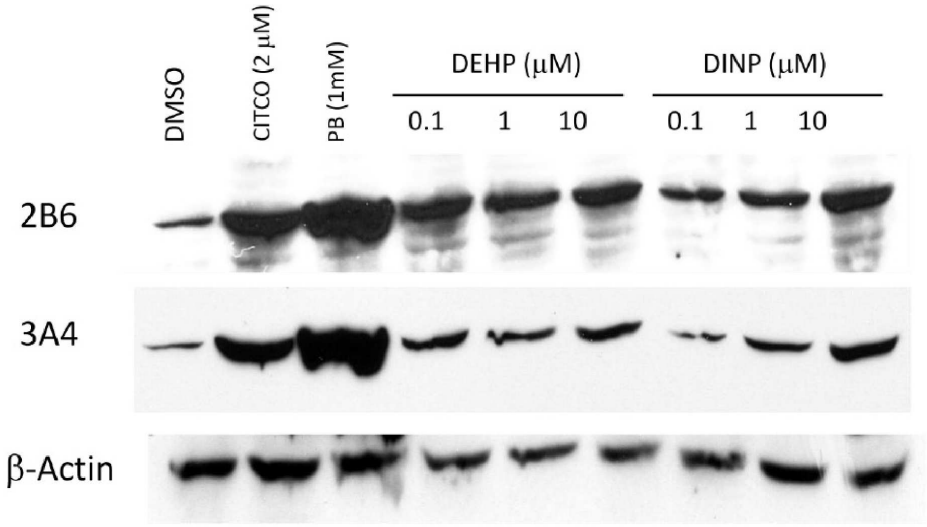

Figure 5. Representative immunoblot showing expression of CYP2B6 and CYP3A4 in human hepatocytes treated with DEHP or DiNP. Human hepatocytes were treated with varying concentrations of DEHP and DiNP with DMSO, PB, and CITCO as controls for 48 h. Protein (S9 fractions) were isolated from lysed cells and subjected to immunoblot analysis with CYP2B6 or CYP3A4-specific antibodies. Actin is shown for normalization of protein loading.
252x143mm (600 x 600 DPI)

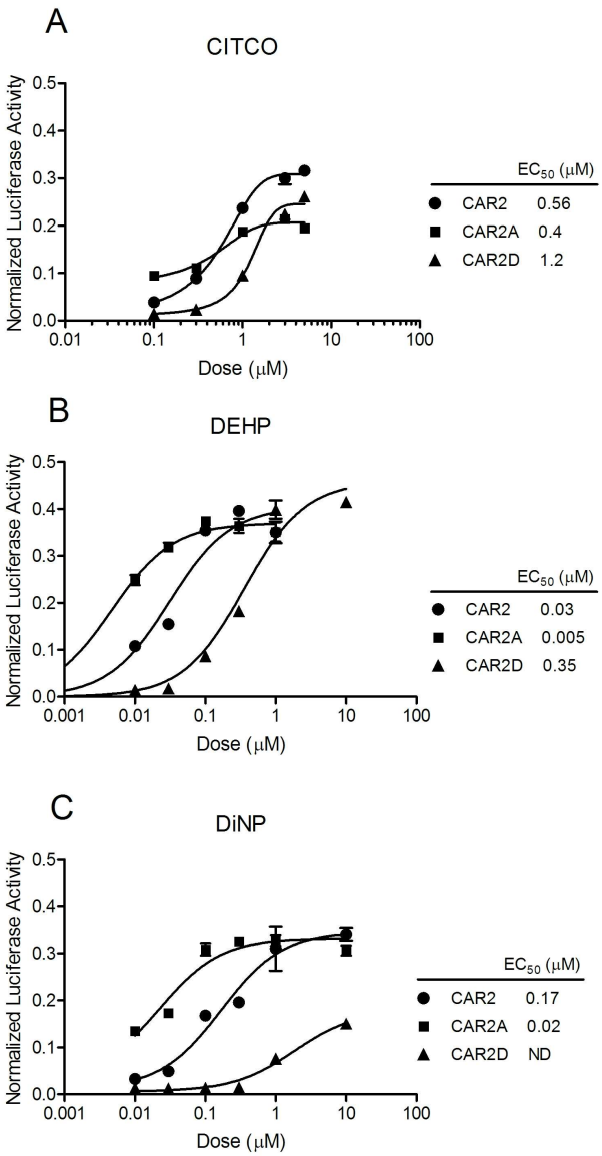

Figure 6. Activation of the 2B6-XREM-PBREM reporter by CAR2, CAR2A, and CAR2D in response to CITCO, DEHP and DiNP. All transfections included the 3.1-RXRα expression vector, the 2B6-XREM-PBREM reporter, the pRL-CMV vector for normalization of transfection efficiency and either CMV2-CAR2 or CMV2-CAR2A. Cells were treated for 24 h. Data are represented as normalized luciferase values and each data point represents the mean (+/- S.E.M.) of quadruplicate treatment wells from a representative transfection experiment.
136x250mm (300 x 300 DPI)

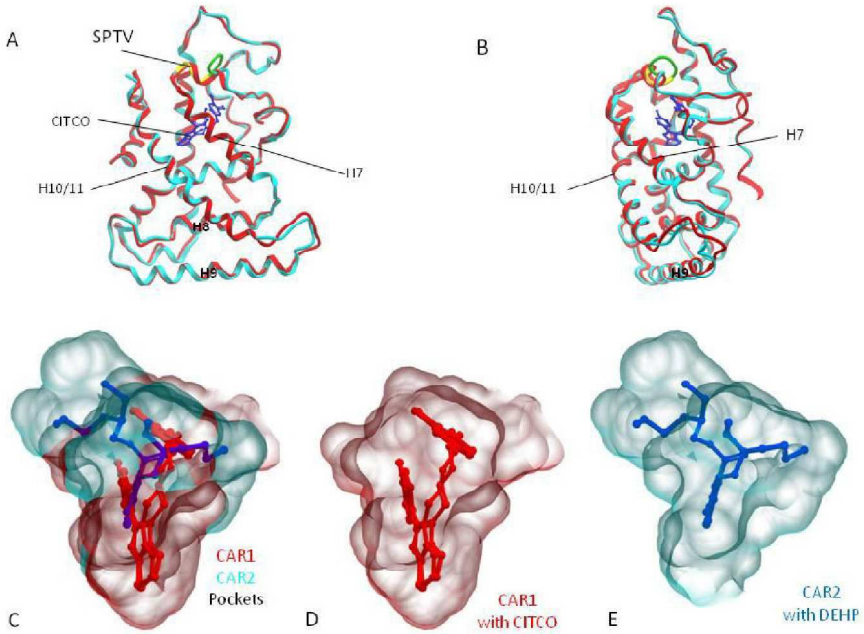

Figure 7. CAR2 predicted protein structure and CAR1 and CAR2 ligand binding pocket models. Panels A and B show two views the Phyre homology model of the human CAR2 receptor ligand binding domain (aqua) superimposed on the CAR1 ligand binding domain structure (red). CITCO (blue) is shown in the ligand binding pocket of CAR1. The CAR2 SPTV insertion is shown in yellow and a region adjacent to the insertion where the structure deviates from CAR1 is shown in green. Panel C shows an overlay of PocketFinder computer generated models of the CAR1 (red) and CAR2 (aqua) LBP with their respective ligands, CITCO (red) and DEHP (blue). Panel D and E show the individual CAR1 and CAR2 LBP.
268x184mm (600 x 600 DPI)